



Estimating phytoplankton stoichiometry from routinely collected monitoring data

Lester L. Yuan · John R. Jones

Received: 4 August 2021 / Accepted: 4 April 2022

This is a U.S. government work and not under copyright protection in the U.S.; foreign copyright protection may apply 2022

Abstract Accurately estimating the elemental stoichiometry of phytoplankton is critical for understanding biogeochemical cycles. In laboratory experiments, stoichiometric ratios vary among species and with changes in environmental conditions. Field observations of total phosphorus (P) and total nitrogen (N) collected at regional and national scales can supplement and expand insights into factors influencing phytoplankton stoichiometry, but analyses applied to these data can introduce biases that affect interpretations of the observed patterns. We introduce an analytical approach for estimating the ratio between phytoplankton N and P from the particulate fraction of nutrient pools in lake samples. We use Bayesian models to represent observations of particulate P and N as the sum of contributions from nutrients bound within phytoplankton and nutrients associated with

non-phytoplankton suspended sediment. Application of this approach to particulate nutrient data collected in Missouri impoundments yields estimates of the mass ratio of N:P in phytoplankton ranging from 8 to 10 across a variety of lakes and seasons. N:P in particulate matter ranged from 6 to 70, a variability driven by differences in nutrients bound to non-phytoplankton suspended sediment. We adapted the Bayesian models to estimate N:P using more commonly available measurements of total P and total N and applied this model to a continental-scale monitoring data set. We compared phytoplankton nutrient content estimated from the two analyses and found that when datasets lack direct measurements of particulate nutrient concentrations, the model estimate of phytoplankton nutrient content includes contributions from nutrients within phytoplankton and dissolved nutrients that are associated with changes in phytoplankton biomass.

Responsible Editor: Ishi Buffam

Supplementary Information The online version contains supplementary material available at <https://doi.org/10.1007/s10533-022-00926-8>.

L. L. Yuan (✉)
Office of Water, U.S. Environmental Protection Agency,
1200 Pennsylvania Ave, NW, Mail code 4304T,
Washington, DC 20460, USA
e-mail: yuan.lester@epa.gov

J. R. Jones
School of Natural Resources, University of Missouri,
Columbia, USA

Keywords Lake · Nitrogen · Phosphorus · Phytoplankton · Redfield ratio · Stoichiometry

Introduction

Phytoplankton provide a critical link in global biogeochemistry cycles, taking up and converting elemental nutrients to forms that are accessible to other trophic levels (Falkowski 1994). Elemental stoichiometry within phytoplankton is a key parameter for

understanding this process, and stoichiometry has long been assumed to conform to a nearly constant ratio among carbon, nitrogen, and phosphorus (Redfield 1958). However, departures from this ratio occur (Geider and Roche 2002) and improved understanding of the reasons for variation in elemental stoichiometry would inform both models of global nutrient cycles and predictions of the local effects of nutrient enrichment.

Wide variations in ratios among C, N, and P in phytoplankton have been observed when environmental conditions are experimentally manipulated. Stoichiometry varied when single algal species were grown in chemostats and the ratio of supplied nutrients (Rhee 1978) or growth rates (Goldman et al. 1979) were varied. Similar studies have examined the effects of environmental factors such as temperature and light availability on stoichiometry (Dickman et al. 2008; Thrane et al. 2017). Analyses of data compiled from individual studies have provided insight into the broader mechanisms and factors influencing stoichiometry (Hillebrand et al. 2013; Yvon-Durocher et al. 2015). These data have also guided the development of models that predict bulk, emergent assemblage characteristics based on phytoplankton traits (Bonachela et al. 2016). Changes in bulk assemblage characteristics with different levels of nutrient supply have also been examined directly with experimental manipulations in microcosms and mesocosms (Hall et al. 2005; Schulhof et al. 2019).

Analyses of large, observational data sets can test stoichiometry theories derived from smaller scale experiments and potentially extend the range of conditions to which these theories apply. Analyses of marine particulate matter showed broad regional differences in stoichiometric ratios (Copin-Montegut and Copin-Montegut 1983), latitudinal gradients (Martiny et al. 2013a; Yvon-Durocher et al. 2015), and temperature effects (Martiny et al. 2013b). Fewer examples of analyses of particulate matter in freshwater lakes are available, but these studies show particulate N:P to be systematically greater than that observed in oceans (Hecky et al. 1993; Sterner et al. 2008). At least two issues inherent to stoichiometric analyses of particulate matter influence the broad applicability of these results. First, relatively few measurements of particulate matter in lakes are available, and therefore, broad-scale analyses require data assembled from distinct sources. However, the effects

of various measurement protocols employed in different surveys have not been considered (Lampman et al. 2001; Gibson et al. 2015). Second, the stoichiometry of all particulate matter differs from that of just phytoplankton because of contributions from non-living suspended sediment with different concentrations of P and N. Hence, stoichiometric trends estimated from lake particulate matter may be biased (Hessen et al. 2003; Yuan and Jones 2019).

Here, we describe a statistical approach for estimating separate contributions of distinct types of particulate matter to measurements of total P (TP) and total N (TN). When applied to particulate matter data, this approach separately accounts for contributions of P and N bound to inorganic and organic sediment and P and N bound in phytoplankton, facilitating a clearer interpretation of observed trends. We hypothesize that the approach can be adapted for use with measurements of TP and TN, rather than just particulate matter measurements, and that estimates of P- and N-content of phytoplankton based on analysis of TP and TN will be similar to estimates based on analysis of particulate matter. By expanding beyond infrequently collected particulate matter measurements to more commonly available lake monitoring measurements of total nutrient pools, phytoplankton stoichiometry can potentially be estimated in a broader array of settings, enhancing efforts to examine the effects of different environmental factors on stoichiometry. We demonstrate the analytical approach with particulate data collected from impoundments in Missouri (Mo) and then test whether similar concentrations of P- and N-content of phytoplankton are estimated when the adapted model is applied to continental spatial scale data collected by the National Lakes Assessment (NLA) (US EPA 2010).

Methods

Data

In 2004 weekly samples were collected from 15 Mo impoundments as integrated photic zone samples near the dam of each reservoir. Study reservoirs were constructed in the Central Irregular Plains region [Ecoregion 40, Omernik (1987)] of northern Mo between 1950 and 1992. The range in size (10–408 ha), mean depth (1.6–5.7 m) and flushing rate (0.1–3.4 times

per year) represent regional reservoir conditions (Jones et al. 2008). Total suspended solids (TSS) were determined by filtering a known volume of lake water through Whatman934-AH filters (nominal filter size: 1.5 μm) that were pre-rinsed, dried, ashed, and tared. Non-volatile suspended sediment (NVSS) was determined by weight after ashing TSS samples, and volatile suspended sediment (VSS) was determined by difference (TSS – NVSS). Samples were analyzed for Chl (uncorrected for degradation products), TP, dissolved P, TN, dissolved inorganic N (DIN), and dissolved organic N (DON). Chl was measured from material retained on a 1 μm Gelman AE filter. Dissolved nutrient concentrations were estimated in filtrate through the Whatman934-AH filters.

NLA data were collected in summers 2007 and 2012 (May–September) from a random sample of lakes in the continental United States. In 2007, lakes with surface areas larger than 4 hectares and, in 2012, lakes larger than 1 hectare, were selected from the contiguous U.S. using a stratified random sampling design (US EPA 2012a). During each visit to a selected lake, an extensive suite of abiotic and biological variables was measured. Only brief details on sampling protocols are provided here regarding the parameters used; more extensive descriptions of sampling methodologies are available in the NLA documentation (US EPA 2007, 2011). A sampling location was established in open water at the deepest point of each lake (up to a maximum depth of 50 m [m]) or in the mid-point of reservoirs. A vertical, depth-integrated methodology was used to collect a water sample from the photic zone of the lake (to a maximum depth of 2 m). Multiple sample draws were combined in a rinsed, 4-L (L) cubitainer. When full, the cubitainer was gently inverted to mix the water, and an aliquot was taken as the water chemistry sample. That subsample was placed on ice and shipped overnight to the Willamette Research Station in Corvallis, Oregon.

TN, TP, nitrate–nitrite (NO_x), ammonia, and dissolved organic carbon (DOC) concentration were measured in the laboratory from the open water sample at prespecified levels of precision and accuracy (US EPA 2012b). Typical laboratory methods included persulfate digestion with colorimetric analysis for TN and TP, and UV promoted persulfate oxidation to CO_2 with infrared detection for DOC. To measure chlorophyll *a* (Chl *a*) concentration, 250 mL of lake water was pumped

through a glass fiber filter in the field and quantified in the laboratory by fluorometry to prespecified levels of precision and accuracy. Examples of lower reporting limits include 4 $\mu\text{g/L}$ for TP, 20 $\mu\text{g/L}$ for TN, 0.2 mg/L for DOC, and 0.5 $\mu\text{g/L}$ for Chl *a*.

Statistical analysis

We specified separate statistical models for phosphorus and nitrogen. For each of these nutrients, we first fit a model to describe particulate concentrations of the nutrient using measurements collected from Mo lakes. We then adapted the particulate nutrient model such that it could be applied to measurements of total nutrients, and applied this adapted model to continental-scale measurements of TP and TN.

Phosphorus

Measurements of particulate P are expressed as the sum of P bound within phytoplankton and P bound to other types of inorganic and organic suspended sediment (i.e., non-phytoplankton suspended sediment, SS_{np}) (Fig. 1):

$$P_{part} = TP - P_{diss} = d_1 Chl^n + d_2 SS_{np}^m \quad (1)$$

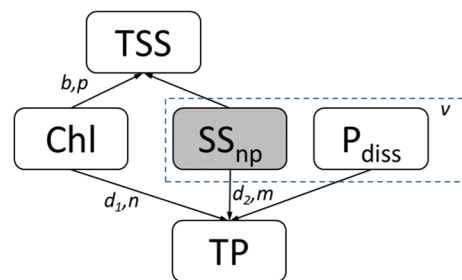


Fig. 1 Schematic for total phosphorus (TP) model. TP in Missouri (Mo) dataset is modeled as being the sum of contributions from P associated with phytoplankton biomass, quantified as chlorophyll concentration (Chl), P sorbed onto non-phytoplankton suspended sediment (SS_{np}), and dissolved P (P_{diss}). The parameters d_1 and n characterize the amount of P per unit of Chl, and the parameters d_2 and m characterize the amount of P per unit of SS_{np} . The box for SS_{np} is shaded to indicate that it is estimated from observations of total suspended sediment (TSS). A similar model for TP is specified for the National Lakes Assessment (NLA) dataset but the contribution from the components enclosed by the dashed rectangle is represented by the parameter v

where particulate P (P_{part}) is calculated as the difference between TP and dissolved P (P_{diss}). P bound within phytoplankton is modeled as the proportion of P_{part} that increases systematically with increases in phytoplankton biomass, as quantified by Chl. This systematic increase is modeled as a power function defined by a coefficient, d_1 , and an exponent, n . P bound to non-phytoplankton sediment is modeled as the proportion of P_{part} that increases systematically with SS_{np} , and this relationship is also expressed as a power function with a coefficient, d_2 , and an exponent, m .

SS_{np} is difficult to measure but a measurement of total suspended solids (TSS) includes contributions from both phytoplankton and non-phytoplankton components. We can therefore estimate SS_{np} by subtracting the contribution of suspended sediment that is directly associated with phytoplankton from TSS. That is, we write the following expression:

$$TSS_{mn} = bChl^p + SS_{np} \quad (2)$$

where TSS_{mn} is the mean value of observed TSS in a sample, and suspended sediment that is directly associated with phytoplankton is again modeled as a power function of Chl concentration, with a coefficient, b , and an exponent, p . Measurements of TSS and Chl were highly skewed, and log transformations were required to effectively fit the relationship to observed data:

$$\log(TSS_i) = \log(b_{j|i}Chl_i^p + SS_{np,i}) + e_{TSS,i} \quad (3)$$

where the subscript, i , refers to measurements in different samples. The coefficient, b , is subscripted by j to indicate that different values are estimated for each month of the year. That is, different amounts of suspended sediment were attributed to phytoplankton depending on when the sample was collected (see Appendix S1: Fig. S1). The term, $e_{TSS,i}$, quantifies measurement error for TSS and was modeled as a normally distributed random error with a mean of zero and a standard deviation of s_{TSS} . The average magnitude of the measurement error for TSS was approximately 10% of the observed value (US EPA 2012b), and because the measurements were log-transformed, this error was expressed as a prior distribution for s_{TSS} that was normal with a mean value of 0.1.

SS_{np} is modeled as a log-normal random variable, and the value of SS_{np} estimated for each sample is used simultaneously in the model for TP during model fitting. Log-transformations are also applied to the TP model equation, yielding the following expression:

$$\log(TP_i) = \log\left(P_{diss,i} + d_{1,j|i}Chl_i^n + d_{2,k|i}SS_{np,i}^m\right) + e_{TP,i} \quad (4)$$

where i indexes individual samples. The random error $e_{TP,i}$ is normally distributed with a mean of zero and a standard deviation of s_{TP} . Measurement error for TP was also 10% of the measured value, and so, a normal prior distribution was specified for s_{TP} with a mean value of 0.1.

We considered the possibility that the P-content in phytoplankton varied seasonally or spatially among lakes by fitting models in which we estimated different values of d_j for each month of the year or for each lake. We also fit models in which values of d_2 (the phosphorus bound to SS_{np}) varied by month or by lake. The inclusion of indices j and k in the equation above indicates that different values for these coefficients were considered. In all, we fit four versions of the model for TP in which either d_1 or d_2 varied by month or lake. Model performance for each of the four versions of the model was quantified by computing the root mean square prediction (RMS) error for $\log(TP)$. Modeled relationships for TSS and TP were fit simultaneously in a hierarchical Bayesian network (Stan Development Team 2016). Weakly informative priors were specified for all parameters except for the parameters quantifying the magnitude of measurement error, which are described above.

The structure of the model described in Eq. 1 provides the basis for estimating a relationship between Chl and P in data sets without direct measurements of particulate P. More specifically, we estimated the relationship between Chl and P by fitting the following relationship to the NLA data:

$$TP = d_1Chl^n + v \quad (5)$$

where the contributions of P_{diss} and SS_{np} to TP are combined in the variable, v . Again, when fitting to the observed NLA data, log transformations are needed:

$$\log(TP_i) = \log(d_1Chl_i^n + v_i) + e_{TP,i} \quad (6)$$

where v_i is a random, log-normally distributed variable, and $e_{TP,i}$ is a normally distributed measurement error with a mean value of zero and a standard deviation of s_{TP} . Different mean values for v_i were calculated for each Level III ecoregion (Omernik 1987) to account for the effects of geographic location on the magnitude of other contributors to TP:

$$v_i = \log\text{Normal}(\mu_{j|i}, \sigma) \quad (7)$$

where μ_j is the mean value for v_i in ecoregion j , and σ is the standard deviation about the ecoregion mean. The individual values of μ_j are themselves drawn from a common normal distribution with a single overall mean and standard deviation.

Intuitively, estimating the values of two random variables in the model (v_i and $e_{TP,i}$) for every sample would overfit the available data. However, two characteristics of the model yield a tractable solution. First, when fitting the model, the value of the standard deviation of $e_{TP,i}$ (s_{TP}) quantifies the location of the limiting Chl-P relationship relative to the edge of the distribution of samples. This parameter is a direct estimate of the average magnitude of measurement error in TP, which is known to be approximately 10% of the measured value (US EPA 2012b). We therefore specified a prior distribution for s_{TP} that was a normal distribution with a mean value of 0.1 (as is specified in the Mo model). Second, because the random variable v_i is log-normally distributed, its value is strictly positive. Therefore, the random values of v_i only account for deviations in the values of TP above the lower bound defined by Chl-P relationship. Taken together, this modeling approach provides a means of estimating the Chl-P relationship that incorporates knowledge regarding both the measurement error in TP and the functional form of the governing relationship.

We restricted NLA data to Chl concentrations corresponding to the 1st and 99th percentiles of the distribution of Chl concentrations observed in Mo, to help ensure that Chl-P relationships were estimated for the same range of eutrophication status in the two data sets. We then fit the model described in Eq. 6 to NLA data and compared the Chl-P relationship estimated from the NLA data to that estimated from the Mo particulate data.

Nitrogen

The format of the model for N in particulate matter in Mo mirrors the model for P in that TN is modeled as the sum of contributions from dissolved N (DIN and DON), N bound in phytoplankton, and N bound to non-phytoplankton sediment (Fig. 2):

$$\log(TN_i) = \log(DIN_i + DON_i + f_{1,j}Chl_i^a + f_{2,k}VSS_{np,i}^b) + e_{TN,i} \quad (8)$$

N bound in phytoplankton is again modeled as a power function of Chl, with a coefficient, f_1 , and an exponent, a ; and N bound in sediment is modeled as a power function of VSS_{np} with a coefficient, f_2 , and an exponent b . The subscript, i , refers to different samples, and coefficients f_1 and f_2 are indexed with j and k again, to indicate that four variations of the TN model were examined in which different values of these coefficients were estimated for each lake or each sampling month. The random error $e_{TN,i}$ is modeled as a normal distribution with a mean of zero and a standard deviation of s_{TN} . Here again, a 10% measurement is expected, and so we specified a normal prior distribution for s_{TN} with a mean value of 0.1. Prior distributions for f_1, f_2, a , and b were weakly informative.

In the model for N, the contribution of suspended sediment to TN is restricted to N bound in VSS, rather than all suspended sediment, because previous analysis and observations have shown that negligible amounts of N are sorbed to inorganic sediment

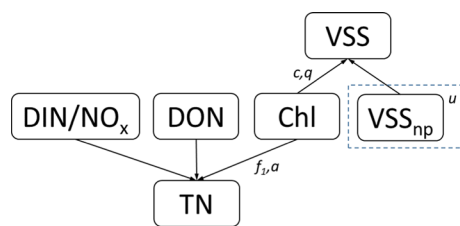


Fig. 2 Schematic for total nitrogen (TN) model. TN in the Mo dataset is modeled as the sum of contributions from dissolved inorganic nitrogen (DIN), dissolved organic nitrogen (DON), N associated with phytoplankton biomass (Chl), and N associated with non-phytoplankton volatile suspended sediment (VSS_{np}). The parameters f_1 and a characterize the amount of N per unit of Chl. A similar model for TN is specified for the NLA dataset but the contribution from the component enclosed by the dashed rectangle is represented by the parameter u . Also, concentrations of NO_x in the NLA data are used to approximate DIN, and DON is modeled as being directly proportional to dissolved organic carbon

(Vitousek and Howarth 1991). Focusing on VSS eliminates the uncertainty introduced by large variations in inorganic suspended sediment that do not affect TN concentrations. A model identical to that used to estimate SS_{np} in the P model was specified to estimate VSS_{np} for the N model.

$$\log(VSS_i) = \log(cChl_i^q + VSS_{np,i}) + e_{VSS,i} \quad (9)$$

The contribution of Chl is modeled as a power function with a coefficient, c , and an exponent, q . The model calculates VSS_{np} as the difference between observed VSS and the component of VSS that is directly associated with changes in Chl. The prior distribution of the standard deviation of $e_{VSS,i}$ was specified as normal with a mean of 0.1. Prior distributions for all other parameters were non-informative. Modeled relationships for VSS and TN were again fit simultaneously as a hierarchical Bayesian network for Mo observations, and the RMS prediction error for each of the variations of the model was computed.

Adapting the particulate N model to measurements available in the NLA was more complex than the model for TP because of the large and consistent contributions of dissolved organic nitrogen (DON) to measurements of TN (Yuan and Jones 2019). Therefore, even in a large dataset such as the NLA, we expected few samples in which the contribution of DON was small relative to N bound to phytoplankton. Direct measurements of DON are rarely collected in routine monitoring; the NLA data set is a typical example of a case in which only TN and NO_x are available. Measurements of DOC, however, are more commonly available, and because DOC and DON often originate from the same allochthonous or autochthonous sources (Berman and Bronk 2003), we hypothesized that DON concentration could be modeled as being proportional to the DOC concentration in a sample. We therefore specified the following model for TN for the NLA data:

$$TN = NO_x + gDOC + f_1Chl^a + u \quad (10)$$

where the contribution of DIN is represented by a direct measurement of NO_x and a second term, $gDOC$, reflects the hypothesis that DON is directly proportional to DOC. The contribution of N bound in phytoplankton is again represented by a power law relationship with Chl with a coefficient, f_1 , and an exponent, a . The final term, u , quantifies the

contribution from N associated with non-phytoplankton VSS. Log-transformation yields the following relationship:

$$\log(TN_i) = \log(NO_{x,i} + g_jDOC_i + f_1Chl_i^a + u_i) + e_{TN,i} \quad (11)$$

where the subscript, i , refers to different samples. The subscript j is included for the coefficient g to indicate that different values for this coefficient were estimated for different Level III ecoregions in the U.S. to account for potential spatial differences in how DOC and DON are related. The random variable u_i is log-normally distributed, and the random error $e_{TN,i}$ is normally distributed with a mean of zero and a standard deviation of s_{TN} . As with the NLA TP model, a prior distribution for s_{TN} is specified with a mean value of 0.1 to represent a 10% average magnitude of measurement error for TN.

We fit the adapted model for TN using the NLA data. Then, to partially validate the hypothesis that DOC and DON were proportional to one another, we tested whether the DOC-DON relationship estimated from the NLA data for the Irregular Plains ecoregion matched the distribution of direct measurements of DOC and DON in the Mo dataset. We then compared the Chl-N relationship estimated using the NLA data to the same relationship estimated using Mo particulate data.

Results

A total of 720 samples collected from 15 impoundments were available for fitting models for P and N in Mo with Chl concentrations ranging from 1 to 195 $\mu\text{g/L}$ (Table 1). NLA data were constrained to samples with Chl concentrations ranging from 1 to 108 $\mu\text{g/L}$, corresponding to the 1st and 99th percentiles of the distribution of Mo Chl measurements. This constraint yielded a total of 2112 samples collected from 1632 different lakes.

In the Mo data set, the tested models differed in their predictive power (Table 2). Lake-specific coefficients for the P-content of SS_{np} yielded the best predictive performance for the P model, whereas month-specific coefficients for the N-content of VSS_{np} yielded the best predictive performance for the N model. Differences in predictive performance among

Table 1 Summary statistics for Mo and NLA data

	Mo			NLA		
	Minimum	Median	Maximum	Minimum	Median	Maximum
Chl ($\mu\text{g/L}$)	0.6	12.1	195.2	1.0	8.0	107.2
TP ($\mu\text{g/L}$)	6.3	33.0	251.8	3.0	35.0	3346.0
TN ($\mu\text{g/L}$)	210	840	2210	14	610	54,000

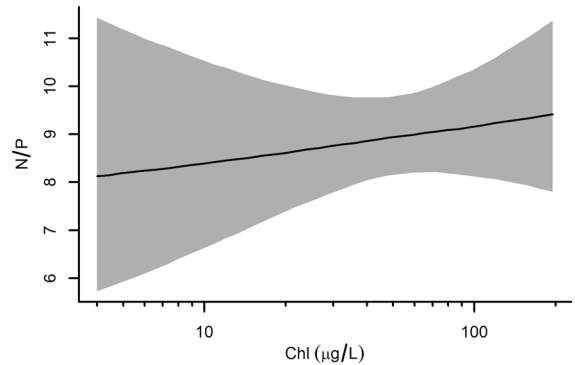
Table 2 RMS error for different model variations

Coefficients for Chl	Coefficients for suspended sediment	TP	TN
–	Lake	0.128	0.556
–	Month	0.166	0.538
Lake	–	0.133	0.553
Month	–	0.162	0.546

the model variations were smaller for the N model compared to the P model.

For the Chl-P relationship, the mean value of the coefficient, d_1 , was estimated as 0.84 (0.61, 1.15) (95% credible interval shown in parentheses), and the exponent, n , was estimated as 0.92 (0.85, 1.01). For the Chl-N relationship, the mean value of the coefficient, f_1 , was estimated as 6.39 (3.81, 10.6), and the exponent, a , was estimated as 0.96 (0.84, 1.09). The mass ratio between N and P within phytoplankton ($N:P_{\text{phyt}}$) can be calculated from the two models as the ratio of N-content per unit of Chl to P-content per unit of Chl (i.e., $N:P_{\text{phyt}} = f_1 \text{Chl}^a / d_1 \text{Chl}^n$). Posterior sampled distributions of f_1 , a , d_1 , and n can then be combined to calculate a posterior distribution of $N:P_{\text{phyt}}$. The mean value of $N:P_{\text{phyt}}$ varied slightly with Chl concentration, but this relationship was not statistically different from a constant with a value between 8.2 and 9.8 (Fig. 3). For comparison, the median value of TN:TP in the Mo dataset was 23 and ranged from 6 to 70.

The amount of P associated with SS_{np} varied considerably among lakes in the Mo data. The overall mean value of the coefficient, d_2 , was 6.84 (5.11, 9.19), but among lakes the value of the coefficient ranged from 2.95 to 17.4. The value of the exponent, m , for this term was 0.50 (0.45, 0.55). We explored the associations between different lake physical characteristics and the P-content of non-phytoplankton sediment and found P-content increased with flushing rate (Fig. 4, left panel). Among Mo samples, the

**Fig. 3** $N:P_{\text{phyt}}$ estimated as a function of Chl. Solid line: mean relationship, gray shading: 90% credible interval

mean contribution of P bound to non-phytoplankton sediment to TP was 37% and ranged from 5 to 81%.

The best model for N included month-specific values for the amount of N associated with VSS_{np} . The overall mean value of the coefficient, f_2 , was 93.6 (75.0, 112), and among different months, the mean value ranged from 52.1 to 152. The value of the exponent, b , was estimated as 0.28 (0.20, 0.38). The N-content of VSS_{np} exhibited a weak relationship with time, increasing in the summer (Fig. 4, right panel).

The estimated mean relationship between Chl and P for the full Mo data set corresponded closely to the lower bound of the observed distribution of samples in the plot of Chl versus P_{part} (Fig. 5, left panel). Contributions to P_{part} from P sorbed to SS_{np} account for the fact that observed values of P_{part} are located above this lower bound. Similarly, the estimated mean relationship between Chl and N for the full Mo data set corresponded with the lower bound of majority of the data (Fig. 5, right panel). Variability in observed values of N_{part} increased as Chl concentration decreased, a trend attributable to the proportional increase in the influence of measurement error when concentrations of N_{part} were less than 100 $\mu\text{g/L}$. That is, as N_{part} decreases

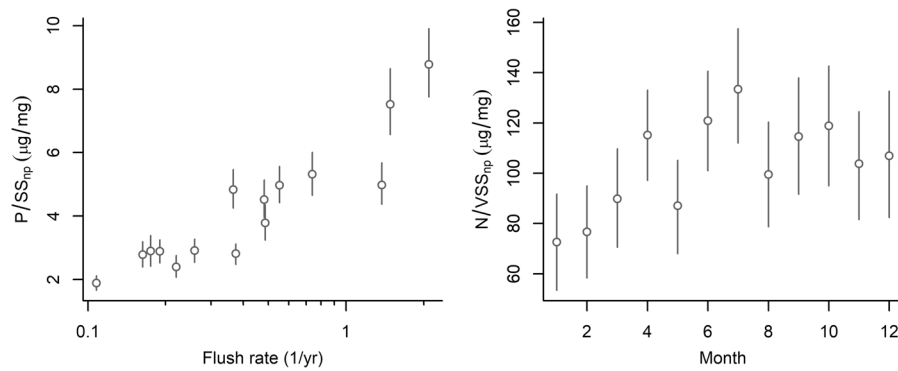
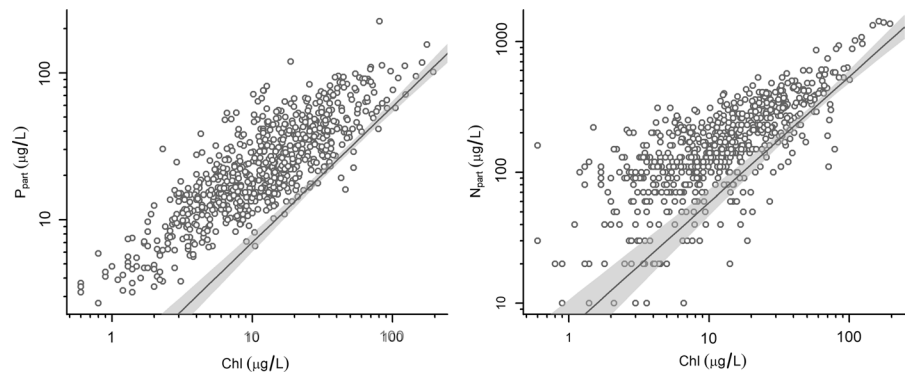


Fig. 4 P-content and N-content of non-phytoplankton sediment and non-phytoplankton volatile suspended sediment, respectively. P-content is plotted versus lake flushing rate, and N-content is plotted versus sampling month. P-content cal-

culated at the overall mean SS_{np} concentration of 3.9 mg/L. N-content calculated at the overall mean VSS_{np} concentration of 0.9 mg/L. Open circles: median value; vertical line segments: 95% credible intervals

Fig. 5 Limiting relationships between Chl and P_{part} (left) and Chl and N_{part} estimated in the Mo data set. Open circles: observed values in Mo data set; solid line: estimated mean relationship for all data; gray shading: 95% credible intervals on overall mean relationship



below 100 $\mu\text{g/L}$, measurement error is estimated as $\pm 10 \mu\text{g/L}$, which is an increasingly large proportion of the observed value. Above 100 $\mu\text{g/L}$, measurement error is estimated as 10% of the measured value, which appears as a constant level of variability in a log-transformed plot.

The adapted model for TP accurately predicted TP concentrations in the NLA with an RMS prediction error of 0.16. The mean value of the exponent, n , in the Chl-P relationship was estimated as 0.96 (0.92, 1.01), and the mean values of the coefficient, d_1 , was 1.16 (0.99, 1.33). Mean ecoregion-specific values for non-phytoplankton contributions to TP ranged widely, from 6 $\mu\text{g/L}$ (in the Appalachians) to 140 $\mu\text{g/L}$ (in upper Midwest ecoregions) (see Appendix S1: Fig. S2). The relationship between Chl and P estimated from NLA closely followed the lower bound of the observed distribution of Chl and TP measurements (Fig. 6, left panel).

The adapted model for TN predicted observed TN concentrations accurately in the NLA, with an RMS prediction error of 0.20. The mean value of the exponent, a , was 1.06 (1.00, 1.12). The mean value of the coefficient, f_1 , was 9.22 (6.73, 12.43). The ratio between DOC and DON ranged from low values of approximately 9 in upper Midwest ecoregions, to high values of approximately 23 in forested ecoregions in the northwest U.S. and in the Appalachian Mountains (Appendix S1: Fig. S3). The relationship between Chl and N estimated from the NLA data was markedly steeper than the lower bound of the observed data and diverged from the observed lower bound at low Chl concentrations (Fig. 6, right panel). This gap between the estimated Chl-N relationship and the lower bound of the data can be attributed to DON, as estimated by DOC. The accuracy of estimated DON in the NLA model was supported by the comparison of direct measurements of DOC and DON in Mo dataset

Fig. 6 NLA data with estimated Chl-P and Chl-N relationships. Open circles: NLA data, solid lines: 95% credible intervals about limiting relationship in NLA, gray shading: 95% credible intervals for relationship estimated in MO

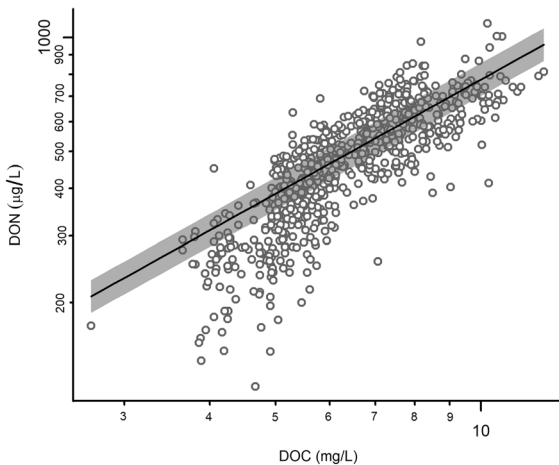
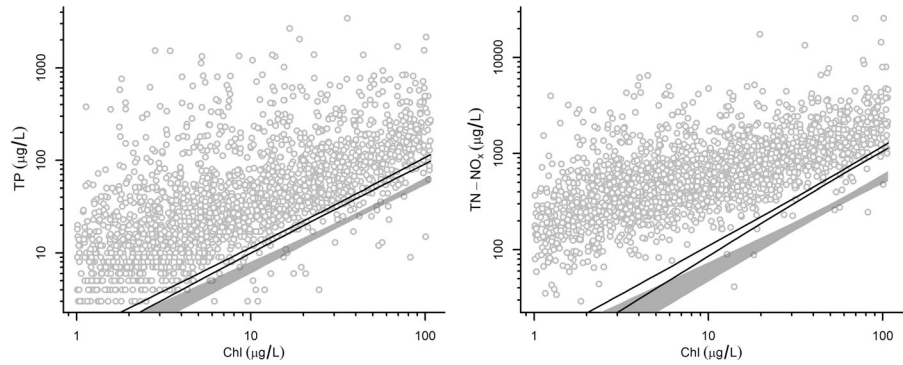


Fig. 7 Measured DOC and DON in Mo dataset. Solid line: estimated relationship between DOC and DON from NLA analysis for Ecoregion 40, the Central Irregular Plains

with parameters estimated from the NLA model for the Central Irregular Plains (where the Mo lakes are located) (Fig. 7). The relationship estimated using NLA data was similar to the mean trends observed in measured DOC and DON in the Mo dataset for DOC concentrations greater than 6 mg/L. However, at lower DOC concentrations, the estimated relationship overpredicted DON, an error that may have introduced a small amount of bias in the estimated relationship between Chl and N in the NLA data.

Estimates of both the Chl-P and Chl-N derived from NLA data were greater than the same relationships estimated from Mo particulate data (Fig. 6). For both nutrients, the values of the exponents on Chl (and the slope of the relationship in the log-log plots) estimated using NLA data were statistically indistinguishable from those estimated using Mo data.

However, the estimated coefficients for both the Chl-P and Chl-N relationships were significantly greater than those estimated with Mo data. $N:P_{\text{phyt}}$ calculated using the results from the NLA model range from 8.4 to 12.1 over the same range of Chl concentrations as shown in Fig. 3.

Discussion

The TP and TN models described here represent total concentrations of each nutrient as the sum of different fractions in the water sample. This approach to modeling TP and TN advances understanding of factors influencing variation in nutrient concentrations in lakes. It also identifies issues inherent to estimating phytoplankton stoichiometry using widely available monitoring data in which particulate P and N are not measured.

Representing measurements of particulate P and N as the sum of phytoplankton and non-phytoplankton components controls for the effects of non-phytoplankton seston when estimating phytoplankton N:P. Field estimates of phytoplankton stoichiometry have traditionally been based on nutrient concentrations in suspended particulate matter, a practice that assumes phytoplankton account for most suspended particles (Hecky et al. 1993). This assumption is more likely true when applied to suspended particles collected in ocean surveys, and analyses of ocean data have yielded insights into factors that affect phytoplankton stoichiometry across broad spatial scales (Martiny et al. 2013b). In lakes, particularly impoundments, the potential for high concentrations of allochthonous suspended sediment weakens the link between particulate and phytoplankton stoichiometry (Yuan and

Jones 2020). Specifically, P adsorbed onto inorganic sediment biases estimates of particulate N:P toward lower values than occur in phytoplankton, while N associated with non-phytoplankton organic sediment can bias particulate N:P to higher values (Hessen et al. 2003). Variations in inorganic and organic sediment concentrations likely account for particulate N:P in lakes being more variable than in oceans (Hecky et al. 1993). In contrast, after controlling for the effects of non-phytoplankton suspended sediment in our analysis, estimates of phytoplankton N:P exhibited relatively little variability, ranging in value from 8 to 10. When N:P is estimated in particulate measurements from lakes with low levels of allochthonous particles, the bias associated with non-phytoplankton sediment may also be small. For example, in 130 particulate samples collected from lakes in the upper Midwest region of North America, mean mass N:P was 9.9, while median N:P was 8.6 (Sterner et al. 2008), values that were very similar to those estimated in the present study.

Analysis of particulate data from the Mo dataset identified factors strongly influencing variation in total concentrations of P_{part} and N_{part} . Differences among lakes in the P-content of SS_{np} accounted for most variability in P_{part} , whereas temporal variability in the N-content of VSS_{np} accounted for most variability in TN models. Substantial amounts of reactive P are adsorbed onto sediment prior to loading into downstream lakes (Zhou et al. 2005), and in the sampled Mo impoundments, our analysis found that P on non-phytoplankton suspended sediment accounted for up to 81% of TP in a single sample. We also found a strong relationship between sediment P-content and flushing rate, a pattern that may have arisen from removal processes that gradually reduce the concentrations of P sorbed to suspended sediment. That is, in rapidly flushed lakes, sediment P-content may reflect concentrations in loaded sediment, whereas in lakes with longer retention times, the observed P-content of SS_{np} may reflect the effects of removal processes (e.g., phytoplankton or bacterial uptake) that occur over longer time scales (DePinto et al. 1981).

Seasonal trends in the N-content of VSS_{np} likely reflect differences in the amount of N in allochthonous organic sediment. During summer, allochthonous sediment likely includes greater amounts of senesced benthic algae (Larsen et al. 2015) and upland sediments during storm events (Fox et al.

2010), both of which would include high N concentrations. In contrast to P, flushing rate was not associated with N-content of VSS_{np} (plot not shown). The lack of an effect of flushing rate on VSS_{np} N-content may reflect the high concentrations of biologically available, inorganic N in the water, which would reduce the need for phytoplankton to use N within VSS_{np} .

These results indicate that temporal and spatial variations in Chl-P and Chl-N relationships (i.e., phytoplankton stoichiometry) accounted for less variability in P_{part} and N_{part} than other sources, but some variations in these relationships are still likely given the extensive evidence from laboratory studies demonstrating the sensitivity of $N:P_{phyt}$ to nutrient availability, light availability, and changes in other environmental conditions (Rhee 1978; Goldman et al. 1979; Dickman et al. 2008; Thrane et al. 2017). Luxury uptake of P may also temporarily alter observed ratios of N:P (Lin et al. 2016). Our estimates of N:Chl and P:Chl may also be influenced by environmental factors that alter Chl:C ratios (Cloern et al. 1995). Temporal trends in Chl-P and Chl-N relationships may be discernible in larger datasets, but the amount of data available in the Mo data limited the degree that temporal and spatial effects could be included in the same model without overfitting.

Alternatively, though, the relative stability of $N:P_{phyt}$ in the present analysis may occur because it represents a bulk, emergent property of the entire phytoplankton assemblage, and less variation in bulk values would be expected relative to N:P estimated for individual species. That is, we may expect that compensatory shifts in phytoplankton assemblage composition occur with changes in environmental conditions that reduce the variability of $N:P_{phyt}$. The stability of $N:P_{phyt}$ may even suggest that some degree of homeostasis exists at the bulk level even though individual phytoplankton species exhibit more variability in their stoichiometry (Elser and Sterner 2002; Hall et al. 2005; Hessen et al. 2013). Applying this same analysis to new datasets of particulate N and P may help broaden our understanding of the conditions under which homeostasis occurs versus conditions in which variations in phytoplankton stoichiometry are important to consider.

TN and TP concentrations are routinely measured in water quality sampling (Soranno et al. 2014), but the lack of concurrent measurements of dissolved N

and P hinders efforts to use these data to understand phytoplankton stoichiometry. Nonetheless, some researchers have investigated trends in these parameters, and conclusions have varied depending on the study scale and location. For example, across three lakes with contrasting catchment land use, patterns in lake TN:TP matched patterns in TN:TP in stream exports to those lakes (Vanni et al. 2011). Similarly, in analyses of nutrient measurements from lakes in Iowa, distinct relationships between row-crop and pasture land use and lake TN:TP were observed (Arbuckle and Downing 2001). In contrast, when patterns were examined in a much larger study area, researchers concluded that the different catchment-scale drivers of TN and TP existed, and therefore, predicting TN:TP stoichiometry from catchment characteristics was not feasible (Collins et al. 2017).

The lack of coherence in the different studies of whole water TN:TP values is not surprising, given that multiple factors influence concentrations in lake water. Considerable variability in the P-content of non-phytoplankton suspended sediment among lakes were observed in our analysis of Mo data, and this variability is compounded by variations in the amount of suspended sediment in a particular lake or region (Jones et al. 2008). At the continental scale, the large range in concentrations of non-phytoplankton P among ecoregions illustrates the magnitude of the effect of sediment bound P on observed TP concentrations. Similarly, whole water TN measurements frequently consist primarily of DON (Yuan and Jones 2019), which also varies substantially among lakes. In certain locations, reactive P and DIN can also contribute substantially to observations of TP and TN (Filstrup and Downing 2017).

Our adaptation of particulate P and N models to more routinely available TP and TN was based on the assumption that in a large enough data set, concentrations of dissolved nutrients and nutrients bound to other suspended sediments would be small enough in some samples to allow an estimate of Chl-P and Chl-N relationships. These attempts were only partially successful. Chl-P and Chl-N relationships estimated from the NLA data had the same slope as estimates based on Mo particulate data, but the coefficients for these relationships were biased toward higher values of P and N per unit of Chl. The similarity of the exponents on these relationships suggests that components of TP and TN are present that

increase with the standing stock of phytoplankton but are in excess of what is bound within phytoplankton. A likely source of these additional nutrients are dissolved concentrations of P and N that are generated by phytoplankton through exudation and lysis (Søndergaard et al. 2000; Prentice et al. 2019). Direct measurements of dissolved P and N in the Mo data supported this interpretation of the model results (see Appendix S1: Fig. S4). Because the adapted model estimates the sum of both dissolved and particulate concentrations of P and N associated with phytoplankton biomass, estimating N:P within only phytoplankton with the current approach is difficult without additional data.

Although the adapted modeling approach does not provide accurate estimates of P and N within phytoplankton, the approach partitions total nutrient concentrations into components that are and are not associated with changes in phytoplankton biomass. In doing so, this approach provides insight into factors influencing observed variation in TP and TN. Similar to the Mo particulate model, much of the variability in TP and TN could be attributed to components other than P and N bound within phytoplankton. For example, in the NLA model for TN, we observed that the amount of DOC associated with a unit of DON varied among ecoregions, a finding that is consistent with observations that the ratio between DOC and DON export is a function of watershed soil characteristics (Aitkenhead-Peterson et al. 2009), watershed runoff (Lewis 2002), vegetation cover, and land use (Willett et al. 2004). The spatial distribution of average DON concentrations also indicated that higher concentrations of DON were observed in lowland lakes than in mountainous lakes, a finding that is consistent with the idea that the rate at which runoff moves through a catchment controls the concentrations of dissolved allochthonous materials (Berman and Bronk 2003; Dillon and Molot 2005). Continental-scale estimates of DON derived from our analysis may also provide initial hypotheses regarding the effects of different catchment factors on the stoichiometry of dissolved organic matter.

In the NLA TP model, we did not attempt to estimate separate contributions from dissolved P and P bound to non-phytoplankton suspended sediment, but previous work has indicated that P bound to SS_{np} accounts for the majority of these contributions (Yuan and Jones 2019, 2020). Hence, regional patterns in the concentrations of

non-phytoplankton P are mainly indicative of variation in both the average amount of inorganic sediment that is delivered to lakes and the amount of P that is bound to this sediment. These regional patterns are similar to those observed in analyses of suspended sediments in streams (Dodds and Whiles 2004), with high contributions of P-bound to suspended sediment in the upper Midwest regions and low contributions in mountainous regions of the eastern and western U.S. The current analytical approach offers a robust means of estimating the impact of suspended sediments to the overall P budgets within lakes over large spatial scales.

The overall analysis described here informs the examination of both particulate and total nutrient measurements. We suggest that this analytical approach provides a means of using field data to investigate trends in stoichiometry at larger spatial scales that would be difficult to address with laboratory studies, helping to broaden and validate the applicability of these studies.

Acknowledgements The authors acknowledge the data collection efforts of the National Lake Assessment sampling teams, and comments provided by G. Kaufman and B. Walsh. Missouri data were collected with support of the Missouri Department of Natural Resources, Missouri Agricultural Experiment Station and Food & Agriculture Policy Research Institute. We specifically thank Daniel Obrecht and Jennifer Graham for data collection and Carol Pollard for analytical work. The views expressed in this paper are those of the authors and do not reflect official policies of the U.S. Environmental Protection Agency.

Funding This research was conducted as part of the author's duties as an employee of the U.S. Environmental Protection Agency.

Data availability Data used in this analysis are publicly available at <https://www.epa.gov/national-aquatic-resource-surveys/data-national-aquatic-resource-surveys>.

Code availability Analyses were conducted with R, a publicly available statistical software. Scripts specific to these analyses will be made available at https://github.com/lesteryuan/tptn_mod.

Declarations

Conflict of interest None to declare.

References

- Aitkenhead-Peterson JA, Steele MK, Nahar N, Santhy K (2009) Dissolved organic carbon and nitrogen in urban and rural watersheds of south-central Texas: land use and land management influences. *Biogeochemistry* 96:119–129. <https://doi.org/10.1007/s10533-009-9348-2>
- Arbuckle KE, Downing JA (2001) The influence of watershed land use on lake N:P in a predominantly agricultural landscape. *Limnol Oceanogr* 46:970–975. <https://doi.org/10.4319/lo.2001.46.4.0970>
- Berman T, Bronk DA (2003) Dissolved organic nitrogen: a dynamic participant in aquatic ecosystems. *Aquat Microb Ecol* 31:279–305. <https://doi.org/10.3354/ame031279>
- Bonachela JA, Klausmeier CA, Edwards KF et al (2016) The role of phytoplankton diversity in the emergent oceanic stoichiometry. *J Plankton Res* 38:1021–1035. <https://doi.org/10.1093/plankt/fbv087>
- Cloern JE, Grenz C, Videgar-Lucas L (1995) An empirical model of the phytoplankton chlorophyll: carbon ratio—the conversion factor between productivity and growth rate. *Limnol Oceanogr* 40:1313–1321. <https://doi.org/10.2307/2838689>
- Collins SM, Oliver SK, Lapierre J-F et al (2017) Lake nutrient stoichiometry is less predictable than nutrient concentrations at regional and sub-continental scales. *Ecol Appl* 27:1529–1540. <https://doi.org/10.1002/eap.1545>
- Copin-Montegut C, Copin-Montegut G (1983) Stoichiometry of carbon, nitrogen, and phosphorus in marine particulate matter. *Deep Sea Res A* 30:31–46. [https://doi.org/10.1016/0198-0149\(83\)90031-6](https://doi.org/10.1016/0198-0149(83)90031-6)
- DePinto JV, Young TC, Martin SC (1981) Algal-available phosphorus in suspended sediments from lower Great Lakes tributaries. *J Gt Lakes Res* 7:311–325. [https://doi.org/10.1016/S0380-1330\(81\)72059-8](https://doi.org/10.1016/S0380-1330(81)72059-8)
- Dickman EM, Newell JM, González MJ, Vanni MJ (2008) Light, nutrients, and food-chain length constrain planktonic energy transfer efficiency across multiple trophic levels. *Proc Natl Acad Sci USA* 105:18408–18412. <https://doi.org/10.1073/pnas.0805566105>
- Dillon PJ, Molot LA (2005) Long-term trends in catchment export and lake retention of dissolved organic carbon, dissolved organic nitrogen, total iron, and total phosphorus: the Dorset, Ontario, study, 1978–1998. *J Geophys Res Biogeosci*. <https://doi.org/10.1029/2004JG000003>
- Dodds WK, Whiles MR (2004) Quality and quantity of suspended particles in rivers: continent-scale patterns in the United States. *Environ Manag* 33:355–367
- Elser JJ, Sterner RW (2002) *Ecological stoichiometry: the biology of elements from molecules to the biosphere*. Princeton University Press, Princeton
- Falkowski PG (1994) The role of phytoplankton photosynthesis in global biogeochemical cycles. *Photosynth Res* 39:235–258. <https://doi.org/10.1007/BF00014586>
- Filstrup CT, Downing JA (2017) Relationship of chlorophyll to phosphorus and nitrogen in nutrient-rich lakes. *Inland Waters* 7:385–400. <https://doi.org/10.1080/20442041.2017.1375176>
- Fox JF, Davis CM, Martin DK (2010) Sediment source assessment in a lowland watershed using nitrogens stable isotopes. *JAWRA* 46:1192–1204. <https://doi.org/10.1111/j.1752-1688.2010.00485.x>
- Geider RJ, Roche JL (2002) Redfield revisited: variability of C:N:P in marine microalgae and its biochemical basis.

- Eur J Phycol 37:1–17. <https://doi.org/10.1017/S0967026201003456>
- Gibson CA, O'Reilly CM, Conine AL et al (2015) Organic matter carbon, nitrogen, and phosphorus from a single persulfate digestion. *Limnol Oceanogr Methods* 13:e10023. <https://doi.org/10.1002/lom3.10023>
- Goldman JC, McCarthy JJ, Peavey DG (1979) Growth rate influence on the chemical composition of phytoplankton in oceanic waters. *Nature* 279:210–215. <https://doi.org/10.1038/279210a0>
- Hall SR, Smith VH, Lytle DA, Leibold MA (2005) Constraints on primary producer n:p stoichiometry along N:P supply ratio gradients. *Ecology* 86:1894–1904. <https://doi.org/10.1890/04-1045>
- Hecky RE, Campbell P, Hendzel LL (1993) The stoichiometry of carbon, nitrogen, and phosphorus in particulate matter of lakes and oceans. *Limnol Oceanogr* 38:709–724
- Hessen DO, Andersen T, Brettum P, Faafeng BA (2003) Phytoplankton contribution to sestonic mass and elemental ratios in lakes: implications for zooplankton nutrition. *Limnol Oceanogr* 48:1289–1296. <https://doi.org/10.4319/lo.2003.48.3.1289>
- Hessen DO, Elser JJ, Sterner RW, Urabe J (2013) Ecological stoichiometry: an elementary approach using basic principles. *Limnol Oceanogr* 58:2219–2236. <https://doi.org/10.4319/lo.2013.58.6.2219>
- Hillebrand H, Steiner G, Boersma M et al (2013) Goldman revisited: faster-growing phytoplankton has lower N:P and lower stoichiometric flexibility. *Limnol Oceanogr* 58:2076–2088. <https://doi.org/10.4319/lo.2013.58.6.2076>
- Jones JR, Obrecht DV, Perkins BD et al (2008) Nutrients, seston, and transparency of Missouri reservoirs and oxbow lakes: an analysis of regional limnology. *Lake Reserv Manag* 24:155–180. <https://doi.org/10.1080/07438140809354058>
- Lampman GG, Caraco NF, Cole JJ (2001) A method for the measurement of particulate C and P on the same filtered sample. *Mar Ecol Prog Ser* 217:59–65. <https://doi.org/10.3354/meps217059>
- Larsen L, Harvey J, Skalak K, Goodman M (2015) Fluorescence-based source tracking of organic sediment in restored and unrestored urban streams. *Limnol Oceanogr* 60:1439–1461. <https://doi.org/10.1002/lno.10108>
- Lewis WM (2002) Yield of nitrogen from minimally disturbed watersheds of the United States. *Biogeochemistry* 57:375–385. <https://doi.org/10.1023/A:1015709128245>
- Lin S, Litaker RW, Sunda WG (2016) Phosphorus physiological ecology and molecular mechanisms in marine phytoplankton. *J Phycol* 52:10–36. <https://doi.org/10.1111/jpy.12365>
- Martiny AC, Pham CTA, Primeau FW et al (2013a) Strong latitudinal patterns in the elemental ratios of marine plankton and organic matter. *Nat Geosci* 6:279–283. <https://doi.org/10.1038/ngeo1757>
- Martiny AC, Vrugt JA, Primeau FW, Lomas MW (2013b) Regional variation in the particulate organic carbon to nitrogen ratio in the surface ocean. *Glob Biogeochem Cycles* 27:723–731. <https://doi.org/10.1002/gbc.20061>
- Omernik JM (1987) Ecoregions of the conterminous United States. *Ann Assoc Am Geogr* 77:118–125. <https://doi.org/10.1111/j.1467-8306.1987.tb00149.x>
- Prentice MJ, Hamilton DP, Willis A et al (2019) Quantifying the role of organic phosphorus mineralisation on phytoplankton communities in a warm-monomictic lake. *Inland Waters* 9:10–24. <https://doi.org/10.1080/20442041.2018.1538717>
- Redfield AC (1958) The biological control of chemical factors in the environment. *Am Sci* 46:230A–A221
- Rhee G-Y (1978) Effects of N:P atomic ratios and nitrate limitation on algal growth, cell composition, and nitrate uptake. *Limnol Oceanogr* 23:10–25. <https://doi.org/10.4319/lo.1978.23.1.0010>
- Schulhof MA, Shurin JB, Declerck SAJ, de Waal DBV (2019) Phytoplankton growth and stoichiometric responses to warming, nutrient addition and grazing depend on lake productivity and cell size. *Glob Change Biol* 25:2751–2762. <https://doi.org/10.1111/gcb.14660>
- Søndergaard M, le B Williams PJ, Cauwet G et al (2000) Net accumulation and flux of dissolved organic carbon and dissolved organic nitrogen in marine plankton communities. *Limnol Oceanogr* 45:1097–1111. <https://doi.org/10.4319/lo.2000.45.5.1097>
- Soranno PA, Cheruvilil KS, Bissell EG et al (2014) Cross-scale interactions: quantifying multi-scaled cause-effect relationships in macrosystems. *Front Ecol Environ* 12:65–73. <https://doi.org/10.1890/120366>
- Stan Development Team (2016) Stan modeling language users guide and reference manual, version 2.14.0. <https://mc-stan.org/users/citations/>
- Sterner RW, Andersen T, Elser JJ et al (2008) Scale-dependent carbon:nitrogen:phosphorus seston stoichiometry in marine and freshwaters. *Limnol Oceanogr* 53:1169–1180. <https://doi.org/10.4319/lo.2008.53.3.1169>
- Thrane J-E, Hessen DO, Andersen T (2017) Plasticity in algal stoichiometry: experimental evidence of a temperature-induced shift in optimal supply N:P ratio. *Limnol Oceanogr* 62:1346–1354. <https://doi.org/10.1002/lno.10500>
- US EPA (2007) Survey of the nation's lakes: field operations manual. Office of Water, U.S. Environmental Protection Agency, Washington, DC
- US EPA (2010) National Lakes Assessment: a collaborative survey of the nation's lakes. Office of Water and Office of Research and Development, Washington, DC
- US EPA (2011) 2012 National Lakes Assessment. Field operations manual. Office of Water, US Environmental Protection Agency, Washington, DC
- US EPA (2012a) 2012 National Lakes Assessment site evaluation guidelines. Office of Water, Washington, DC
- US EPA (2012b) 2012b National Lakes Assessment. Laboratory operations manual. U.S. Environmental Protection Agency, Washington, DC
- Vanni MJ, Renwick WH, Bowling AM et al (2011) Nutrient stoichiometry of linked catchment-lake systems along a gradient of land use. *Freshw Biol* 56:791–811. <https://doi.org/10.1111/j.1365-2427.2010.02436.x>
- Vitousek PM, Howarth RW (1991) Nitrogen limitation on land and in the sea: how can it occur? *Biogeochemistry*. <https://doi.org/10.1007/BF00002772>
- Willett VB, Reynolds BA, Stevens PA et al (2004) Dissolved organic nitrogen regulation in freshwaters. *J Environ Qual* 33:201. <https://doi.org/10.2134/jeq2004.2010>

- Yuan LL, Jones JR (2019) A Bayesian network model for estimating stoichiometric ratios of lake seston components. *Inland Waters* 9:61–72. <https://doi.org/10.1080/20442041.2019.1582957>
- Yuan LL, Jones JR (2020) Rethinking phosphorus-chlorophyll relationships in lakes. *Limnol Oceanogr*. <https://doi.org/10.1002/lno.11422>
- Yvon-Durocher G, Dossena M, Trimmer M et al (2015) Temperature and the biogeography of algal stoichiometry. *Glob Ecol Biogeogr* 24:562–570. <https://doi.org/10.1111/geb.12280>
- Zhou A, Tang H, Wang D (2005) Phosphorus adsorption on natural sediments: modeling and effects of pH and sediment composition. *Water Res* 39:1245–1254. <https://doi.org/10.1016/j.watres.2005.01.026>

Publisher's Note Springer Nature remains neutral with regard to jurisdictional claims in published maps and institutional affiliations.